
2-1-2020

Engineered Fn3 Protein has Targeted Therapeutic Effect on Mesothelin-Expressing Cancer Cells and Increases Tumor Cell Sensitivity to Chemotherapy

Allison R. Sirois
University of Massachusetts Amherst

Daniela A. Deny
Smith College

Yanxuan Li
Smith College

Yacine D. Fall
Smith College

Sarah J. Moore
Smith College, sjmoore@smith.edu

Follow this and additional works at: https://scholarworks.smith.edu/egr_facpubs



Part of the [Engineering Commons](#)

Recommended Citation

Sirois, Allison R.; Deny, Daniela A.; Li, Yanxuan; Fall, Yacine D.; and Moore, Sarah J., "Engineered Fn3 Protein has Targeted Therapeutic Effect on Mesothelin-Expressing Cancer Cells and Increases Tumor Cell Sensitivity to Chemotherapy" (2020). Engineering: Faculty Publications, Smith College, Northampton, MA. https://scholarworks.smith.edu/egr_facpubs/57

This Article has been accepted for inclusion in Engineering: Faculty Publications by an authorized administrator of Smith ScholarWorks. For more information, please contact scholarworks@smith.edu



Published in final edited form as:

Biotechnol Bioeng. 2020 February ; 117(2): 330–341. doi:10.1002/bit.27204.

Engineered Fn3 protein has targeted therapeutic effect on mesothelin-expressing cancer cells and increases tumor cell sensitivity to chemotherapy

Allison R. Sirois^{1,2}, Daniela A. Deny³, Yanxuan Li², Yacine D. Fall³, Sarah J. Moore^{1,2,4,*}

¹Molecular and Cellular Biology Program, University of Massachusetts Amherst, Amherst, Massachusetts, United States of America

²Picker Engineering Program, Smith College, Northampton, Massachusetts, United States of America

³Biochemistry Program, Smith College, Northampton, Massachusetts, United States of America

⁴Department of Biological Sciences, Smith College, Northampton, Massachusetts, United States of America

Abstract

Mesothelin is a protein expressed at high levels on the cell surface in a variety of cancers, with limited expression in healthy tissues. The presence of mesothelin on tumor tissue correlates with increased invasion and metastasis, and resistance to traditional chemotherapies, through mechanisms that remain poorly understood. Molecules that specifically recognize mesothelin and interrupt its contribution to tumor progression have significant potential for targeted therapy and targeted drug delivery applications. A number of mesothelin-targeting therapies are in pre-clinical and clinical development, although none are currently approved for routine clinical use. In this work, we report the development of a mesothelin-targeting protein based on the fibronectin type-III non-antibody protein scaffold, which offers opportunities for applications where antibodies have limitations. We engineered protein variants that bind mesothelin with high affinity and selectively initiate apoptosis in tumor cells expressing mesothelin. Interestingly, apoptosis does not occur through a caspase-mediated pathway, and does not require downregulation of cell-surface mesothelin, suggesting a currently unknown pathway through which mesothelin contributes to cancer progression. Importantly, simultaneous treatment with mesothelin-binding protein and chemotherapeutic mitomycin C had a greater cytotoxic effect on mesothelin-positive cells compared to either molecule alone, underscoring the potential for combination therapy including biologics targeting mesothelin.

Keywords

protein engineering; targeted therapy; cancer; mesothelin; combination therapy

*Corresponding author: Sarah J. Moore, Address: 100 Green St., Smith College, Northampton, Massachusetts 01063, sjmoore@smith.edu, Phone: 413-585-7005; FAX: 413-585-7001.

INTRODUCTION

Mesothelin (MSLN) is a cell surface protein that is overexpressed in numerous cancers, including ovarian (K Chang & Pastan, 1996; Kai Chang, Pastan, & Willingham, 1992, p. 199; Hilliard, 2018), triple negative and other breast (Bayoglu et al., 2015; Hassan et al., 2016; Parinyanitikul et al., 2013; Tchou et al., 2012), lung (Mitchell Ho et al., 2007; Kachala et al., 2014; Thomas et al., 2015, p. 201), liver (Ordóñez, 2003; Yu et al., 2010), pancreatic (Argani et al., 2001; Chen, Hung, Wang, Paul, & Konstantopoulos, 2013; Hassan et al., 2016; Shimizu et al., 2012), and mesothelioma (Servais et al., 2012). The aberrant expression of MSLN is known to promote tumor cell survival, progression, and metastasis in vitro and in vivo (Kai Chang et al., 1992; Gubbels et al., 2006; Rump et al., 2004; Wang et al., 2012). MSLN expression is limited in normal tissue, with only low levels expressed on the mesothelial cells of the pleura, peritoneum, and pericardium (Hassan, Bera, & Pastan, 2004). The role of MSLN in normal development is currently still unknown. Mice with an inactivated *MSLN* gene display no distinct phenotype and are capable of producing healthy offspring, suggesting that MSLN is not essential for mammalian development (Bera & Pastan, 2000). The differential expression pattern between cancer and healthy tissue, and apparent non-essential role for MSLN in normal tissue, makes MSLN a promising biomarker for cancer diagnosis and therapeutic targeting.

Previous studies have proposed a variety of mechanisms by which MSLN promotes tumor progression (Zhewei Tang, Qian, & Ho, 2013). Growing evidence indicates that MSLN aids in cell motility, implantation, and metastasis through its interaction with another tumor surface protein, CA125, also known as MUC16 (Chen et al., 2013; Gubbels et al., 2006; Rump et al., 2004). The interaction of these two cell surface proteins has been observed to facilitate metastasis in ovarian tumors (Hilliard, 2018; Pastan & Hassan, 2014), and promote cancer cell motility and invasion in pancreatic cancer (Chen et al., 2013). The interaction between MSLN and CA125 mediates heterotypic cell adhesion, important for tumor cell invasion and metastasis (Rump et al., 2004). Moreover, blocking the interaction of MSLN and CA125 with anti-MSLN antibodies blocks the observed adhesion (Rump et al., 2004). Overexpression of CA125 has been shown to induce metastasis, but only when mediated by binding to MSLN (Comamala et al., 2011). MSLN expression may also promote cancer cell survival and proliferation through the NF- κ B signaling pathway. MSLN expression in pancreatic cancer cells was correlated with constitutive activation of the transcription factor STAT3, which lead to increased formation of the cyclin E/cyclin-dependent kinase 2 complex, as well as increased G₁-S transitions (Bharadwaj, Li, Chen, & Yao, 2008). Several studies suggest MSLN expression is associated with chemoresistance, and shorter progression-free survival and overall survival (Cheng et al., 2009). MSLN-induced NF- κ B pathway activation has been shown to mediate resistance to several chemotherapeutics through upregulation of anti-apoptotic proteins, including Bcl-2 and Mcl-1 (Bharadwaj, Marin-muller, Li, Chen, & Yao, 2011; M.-C. Chang et al., 2009). Altering MSLN biochemical signaling pathways or interrupting the binding of MSLN and CA125 are viable therapeutic strategies to reduce cancer progression and metastasis.

Promising results from pre-clinical and clinical trials to target MSLN with antibodies, antibody derivatives, immunotoxins, antibody-drug conjugates, and CAR-T cells for therapy

demonstrate the promise of MSLN-targeting methods (El-Behaedi et al., 2018; Golfier et al., 2014; Mitchell Ho, Feng, Fisher, Rader, & Pastan, 2011; Quanz et al., 2018; Z Tang et al., 2013; Adusumilli et al., 2014; Morello, Sadelain, & Adusumilli, 2016). However, no MSLN-targeting molecules are currently approved for routine clinical use. Targeted therapeutics have made significant impacts in cancer treatment, resulting in increased efficacy and reduced toxicity compared to traditional chemotherapies. Novel targeted therapy approaches for MSLN-positive tumors have potential for substantial impact in the clinic for patients who currently do not have a targeted therapy option.

We have recently reported engineering protein variants based on the fibronectin type III (Fn3) non-antibody protein scaffold that bind to MSLN with moderate affinities ($K_D = 100$'s nM) (Sirois, Deny, Baiertl, George, & Moore, 2018). Fn3 variants that specifically bound to MSLN on human cancer cells were internalized, and co-localized to early endosomes, indicating their promise for drug delivery applications. MSLN has been previously shown to readily internalize bound ligands, underscoring the potential of MSLN as a cell-surface target to mediate intracellular drug delivery (Zhang & Pastan, 2012). While antibody-based therapies have found great success for a variety of clinical needs, there are some applications where other protein structures may be advantageous and complement clinical contributions from antibodies, motivating the development of non-antibody protein scaffolds for engineering molecular recognition, including the Fn3 scaffold (Koide, Bailey, Huang, & Koide, 1998; Moore, Leung, & Cochran, 2012; Fiedler & Skerra, 2014; Simeon & Chen, 2018; Vazquez-Lombardi et al., 2015).

Here, we describe further evolved Fn3 variants with enhanced binding affinity for MSLN. Our data show that treatment of MSLN-positive tumor cells with engineered MSLN-binding Fn3 protein has cytotoxic effects on MSLN-expressing cancer cells, leading to tumor cell apoptosis. Our results indicate that apoptosis is by a caspase-independent pathway, and that the cytotoxic effects are not due to downregulation of MSLN on the surface of cancer cells, revealing that a novel signaling pathway is potentially being targeted by the engineered MSLN-binding protein, with implications for future drug development efforts. Importantly, when MSLN-positive cells are simultaneously treated with MSLN-binding Fn3 protein and established chemotherapeutic mitomycin C (MMC), the tumor cells exhibit enhanced sensitivity to the chemotherapeutic agent with increased apoptosis compared to MSLN-positive cells treated with MMC alone. These results highlight the potential of targeting MSLN with biologic therapeutics in combination therapy with traditional chemotherapeutics for selective, synergistic treatment of tumors expressing MSLN.

MATERIALS AND METHODS

Reagents and cell lines

PBSA buffer was composed of phosphate buffered saline (PBS) and 0.1% bovine serum albumin (BSA). A431/H9 cells (gift of M. Ho, National Cancer Institute, 2016) (M. Ho et al., 2005) were cultured in RPMI-1640 supplemented with 10% FBS, 1% penicillin-streptomycin and 700 μ g/mL Geneticin selective antibiotic (G418) (Thermo Fisher). KB-3-1 cells (gift of M. Gottesman, National Cancer Institute, 2016) (Shen et al., 1986) were cultured in DMEM supplemented with 10% FBS and 1% penicillin-streptomycin. T-47D

cells (gift of S. Smith-Schneider, Pioneer Valley Life Sciences Institute, 2019) (Keydar et al., 1979) were cultured in DMEM supplemented with 10% FBS, 0.2 units/mL human insulin (Sigma # I9278-5ML) and 1% penicillin-streptomycin. OVCAR-3 cells (ATCC #HTB-161, 2015) were cultured in RPMI-1640 supplemented with 20% FBS, 1% penicillin-streptomycin, and 0.01 mg/mL human insulin. All cells were grown at 37°C in a humidified atmosphere containing 5% CO₂.

Maturation and evolution of Fn3 variant 3.4.4 by yeast surface display

A Gr2 library that we had previously evolved for MSLN-binding Fn3 variants was further sorted and affinity matured as a third generation library using yeast surface display (Boder & Wittrup, 1997; Sirois et al., 2018). Briefly, following error-prone PCR with nucleotide analogs, the library was sorted twice by magnetic bead selection (MACS) using biotinylated, Fc-tagged recombinant human MSLN (Acro Biosystems #MSN-H826x) followed by a fluorescence activated cell sorting (FACS) selection for full-length clones using an antibody against the C-terminal c-myc epitope tag. Full-length clones were incubated with a chicken anti-c-myc antibody and the biotinylated Fc-tagged MSLN. To increase the sorting stringency, concentrations of MSLN were decreased over four iterative rounds of enrichment, from 20 nM in the first sort to 5 nM in the fourth sort. Cells were washed and incubated with a goat anti-chicken Alexa Fluor 647 (AF647) conjugate and Alexa Fluor 488 (AF488)-conjugated streptavidin. Cells were washed and double-positive yeast cells were collected on a BD BioSciences FACSaria II. Plasmid DNA from the enriched library was recovered using a Zymoprep Yeast Plasmid Miniprep II kit (Zymo Research) following manufacturer's protocol, transformed into bacteria, and individual clones were sequenced by standard Sanger DNA sequencing methods.

Engineered Fn3 protein production and purification

MSLN-binding Fn3 variant 3.4.4 and negative control protein Fn3 RDG, in which the RGD integrin-binding motif has been mutated to RDG (plasmid DNA provided by B. Hackel, University of Minnesota), were prepared as previously described (Sirois et al., 2018). Briefly, Fn3 genes were cloned into a pET vector with a C-terminal hexahistidine tag (plasmid provided by B. Hackel, University of Minnesota) and expressed in BL21(DE3) *E. coli*. Cultures were grown in LB and induced overnight at 20°C with 0.5 mM Isopropyl-β-D-thiogalactopyranoside (IPTG). Cells were resuspended in lysis buffer (35 mM Na₂HPO₄-dibasic, 15 mM NaH₂PO₄-monobasic, 500 mM NaCl, 5 mM CHAPS, 25 mM imidazole, 5% glycerol) supplemented with an EDTA-free protease inhibitor (Pierce), and lysed by repeated freezing and thawing. Soluble fractions were isolated by centrifugation. Fn3 variant 3.4.4 was purified by cobalt affinity chromatography with HisPur cobalt resin (Thermo Fisher) while Fn3 RDG was purified by nickel affinity chromatography with Ni-NTA agarose resin (Thermo Fisher) followed by size exclusion chromatography (SEC) on a Superdex 75 10/300 column (GE Healthcare Life Sciences). Protein samples were analyzed for purity by SDS-PAGE on a BioRad ChemiDoc MP imaging system.

Binding affinity measurements of soluble Fn3 proteins for MSLN-positive tumor cells

A431/H9 and MCF-7 cells were cultured to 80% confluency, as described above, harvested, washed, and pelleted at 200g for 5 min at 4°C. MSLN expression was detected by a mouse

anti-MSLN antibody (clone K1, Abcam, 1:50) and a goat anti-mouse PE conjugate (1:25). Cells were incubated with a range of concentrations of 3.4.4. or Fn3 RDG in a total volume of 50 μ L PBSA for 1 h at 23°C with rotation. Cells were washed with PBSA and incubated with a mouse anti-His₆ DyLight-488 antibody (Abcam #ab117512, 1:50) for 20 min at 4°C and protected from light. Fluorescence was analyzed using an EMD Millipore Guava easyCyte flow cytometer. Mean fluorescence intensities for Fn3 variant binding were determined using InCyte software (EMD Millipore). Data was plotted and fit to a sigmoidal curve using KaleidaGraph software. Dissociation constants (K_D) were determined as the half-maximal value of the sigmoidal fit for three separate experiments, and the mean and standard deviation (SD) for the K_D are reported.

Cell viability measurements

Cell viability was determined using a Cell Counting Kit-8 (CCK-8, Dojindo Laboratories, Japan), according to the manufacturer's instructions. Briefly, cells were seeded at 3×10^3 (KB-3-1) or 5×10^3 (T-47D) cells per well in 96-well plates and cultured overnight in a final volume of 100 μ L of medium. After overnight culture, the medium was exchanged to serum-free medium containing various concentrations of 3.4.4 or Fn3 RDG (2, 20, or 200 nM). As a positive control, cells were treated with 10 μ M mitomycin C (MMC), a known chemotherapeutic agent. At 48 h post treatments, spent media was removed and replaced with 100 μ L of fresh media with 10 μ L of CCK-8 reagent and the cells were incubated at 37°C for an additional 2 h. The absorbance of each well was measured at 450 nm on a Tecan Infinite M100 microplate reader. All treatments were carried out as triplicates in three independent experiments. Data were analyzed using the Magellan 7.0 software (Tecan). Measured absorbance was normalized with absorbance values of the cell culture media that did not contain cells. Untreated cells were regarded as control, and cell viability was calculated as the ratio of the absorbance of test and control wells.

Apoptosis experiments

Apoptosis was determined using a Dead Cell Apoptosis kit with annexin V-AF488 and propidium iodide (PI) (Molecular Probes), according to the manufacturer's instructions. Briefly, KB-3-1 cells were seeded at 2.5×10^5 cells in 35 mm plates and cultured overnight in a final volume of 3 mL of medium. After overnight culture, the medium was exchanged to serum-free medium containing 200 nM of 3.4.4 or Fn3 RDG. At 48 h post treatment, cells were trypsinized, washed three times with PBS, and resuspended in 1X binding buffer to a density of 1×10^6 cells/mL. 100 μ L of this cell suspension was incubated with 5 μ L of the supplied annexin V-AF488 and 1 μ L of PI (100 μ g/mL) for 15 min while protected from light. The percentages of annexin V-AF488-positive and PI-positive cells were determined from the fluorescence of 25,000 cells measured on an EMD Millipore Guava easyCyte flow cytometer. All treatments were carried out as triplicates. Data were analyzed using InCyte software (EMD Millipore).

Caspase-3/7 activation

Caspase induction was assessed using the Caspase-Glo 3/7 assay (Promega), according to the manufacturer's instructions. Briefly, KB-3-1 cells were seeded at 5×10^3 cells per well in 96-well plates and cultured overnight in a final volume of 100 μ L of medium. After

overnight culture, the medium was exchanged to serum-free medium containing 200 nM of 3.4.4 or Fn3 RDG. As a positive control, cells were treated with 10 μ M MMC. At the specific time point of either 6, 12, 24, 36, or 48 h, 100 μ L of Caspase-3/7 reagent was added to each well, gently mixed at 300 rpm for 30 s, and incubated at 23°C for an additional 2 h. Luminescence was measured on a Tecan Infinite M100 microplate reader. All treatments were carried out as triplicates in three independent experiments, unless otherwise noted. Data were analyzed using the Magellan 7.0 software.

Receptor downregulation

KB-3-1 cells were seeded at 3×10^4 cells per well in 96-well plates, grown overnight, and serum starved for 12-16 h. Cells were treated with 200 nM 3.4.4 or Fn3 RDG for the indicated time between 0 and 48 h. Medium was removed and cells were washed with PBS, detached with 0.05% trypsin-EDTA, and placed on ice for the remainder of the assay. Cells were washed with PBSA and incubated with an anti-MSLN antibody raised in mouse for 1 h on ice followed by a goat anti-mouse PE conjugate antibody. Cells were washed and analyzed by flow cytometry. All treatments were carried out in triplicates. Levels of cell surface MSLN expression were determined from the fluorescence of 25,000 cells measured on a EMD Millipore Guava easyCyte flow cytometer. Data were analyzed using InCyte software (EMD Millipore).

Combination therapy with engineered protein variant and MMC

The Dead Cell Apoptosis kit with annexin V-AF488 and propidium iodide (PI) described above was used to determine whether treatment with Fn3 variant 3.4.4 could enhance the susceptibility of MSLN-expressing cells to MMC-induced apoptosis. Briefly, KB-3-1 cells or OVCAR-3 cells were seeded at 1×10^5 cells in 12-well plates and cultured overnight in a final volume of 1 mL of medium. After overnight culture, the medium was exchanged to serum-free medium containing 200 nM Fn3 variant 3.4.4, 1 μ M MMC, or 1 μ M MMC with 200 nM Fn3 variant 3.4.4. At 48 h post treatment, cells were trypsinized, washed three times with PBS, and resuspended in 1X binding buffer to a density of 1×10^6 cells/mL. 100 μ L of this cell suspension was incubated with 5 μ L of the supplied annexin V-AF488 and 1 μ L of PI (100 μ g/mL) for 15 min at 23°C while protected from light. The percentages of annexin V-AF488-positive and PI-positive cells were determined from the fluorescence of at least 20,000 cells measured on an EMD Millipore Guava easyCyte flow cytometer. All treatments were carried out as triplicates. Data were analyzed using InCyte software (EMD Millipore).

Statistical analysis

Statistical differences between groups were determined using an unpaired Student's two-tailed *t*-test. A *p* value of < 0.05 was considered statistically significant (* $p < 0.05$, ** $p < 0.01$, *** $p < 0.001$). All data are presented as mean \pm SD.

RESULTS AND DISCUSSION

Fn3 proteins from further evolved library bind MSLN with high affinity.

Our previously reported MSLN-binding Fn3 proteins were engineered from a naïve yeast surface display Fn3 library (Sirois et al., 2018; Woldring, Holec, Zhou, & Hackel, 2015)

(Fig. 1A, B) and their moderate affinity for cell surface MSLN motivated additional rounds of directed evolution. Following mutagenesis of our second generation library, the third generation library was subjected to two rounds of MACS, a FACS sort for full-length expression and four iterative rounds of dual-color FACS for binding to MSLN. The resultant population yielded enrichment of evident MSLN-binding clones (Fig. 1C). Sequence analysis of individual clones identified three dominant variants: 3.1.6, 3.4.4 and 3.4.5 (Fig. 1D). All three variants included a shared single mutation in the BC binding loop compared to previously reported Fn3 clones 1.4.1 and 2.4.1 (Sirois et al., 2018). Single framework mutations N63K and D3Y are incorporated into clones 3.1.6 and 3.4.4, respectively. In addition to the D3Y mutation, variant 3.4.5 incorporates three further framework mutations, including P64S, S82Y, and D94N. These variants were transformed into EB100 yeast surface display strain and their binding to a range of MSLN concentrations was assessed by flow cytometry (Fig. 1E). From these data, variant 3.4.4 was subsequently selected for further binding and therapeutic characterization.

Soluble Fn3 protein selectively binds the surface of MSLN-positive cancer cells.

Fn3 variant 3.4.4 and the non-binding control, Fn3 RDG, both containing a C-terminal His₆ tag, were solubly produced in *E. coli* and high purity of proteins following metal affinity purification was verified by SDS-PAGE analysis (Fig. 2A). Equilibrium binding titrations of Fn3 variant 3.4.4 and Fn3 RDG on A431/H9 and MCF-7 cell lines were performed (Fig. 2B). The A431/H9 cell line is an A431 human epidermoid carcinoma cell line transfected to stably overexpress MSLN on its surface and MCF-7 is a human breast cancer cell line that does not express MSLN on its surface (K Chang & Pastan, 1996; Mitchell Ho et al., 2011; Sirois et al., 2018). Previously reported Fn3 proteins engineered to bind cell surface MSLN demonstrated moderate binding affinities ($K_D > 400$ nM) (Sirois et al., 2018). The Fn3 variant reported here, 3.4.4, binds to MSLN-expressing A431/H9 cells with a binding affinity of $K_D = 19 \pm 1$ nM, while displaying no binding to the MSLN-negative control cell line, MCF-7. The nonbinding control, Fn3 RDG, also showed no detectable binding to the A431/H9 cell line (Fig. 2B).

Engineered Fn3 protein reduces the viability of MSLN-positive cancer cells.

The effect of Fn3 variant 3.4.4 on cell viability was studied using the CCK-8 assay based on WST-8, a water-soluble tetrazolium salt that is reduced by dehydrogenase to produce a yellow formazan dye. The amount of formazan dye generated by dehydrogenase activity is directly proportional to the number of living cells.

The KB-3-1 cell line is a human cervical carcinoma cell line reported to express moderate levels of MSLN on its surface (Zhang, Xiang, Hassan, & Pastan, 2007), while the T-47D cell line is a human breast carcinoma cell line that is not known to endogenously express MSLN (Uehara, Matsuoka, & Tsubura, 2008). While H9 cells that were transfected to express high levels of MSLN were ideal for binding assays, we chose the endogenously expressing KB-3-1 cells for therapeutic characterization of Fn3 3.4.4. Using an anti-MSLN antibody, high levels of MSLN were confirmed on the surface of KB-3-1 cells, and no MSLN was detected on the surface of T-47D cells (Fig. 3A). We tested the cytotoxic effect of concentrations of 3.4.4 protein based on the measured dissociation constant, selecting to test

concentrations equivalent to the dissociation constant (20 nM) and one order of magnitude above (200 nM) and below (2 nM) the dissociation constant. After 48 h of treatment, Fn3 variant 3.4.4 significantly reduced ($p < 0.05$) the number of viable cells in the KB-3-1 cell line in a dose-dependent manner (Fig. 3B), but did not affect viability of the T-47D cell line (Fig. 3C). The non-binding Fn3 RDG control demonstrated no effect on cell viability for either cell line. In contrast to the MSLN-dependent effect of Fn3 variant 3.4.4, non-targeted chemotherapeutic MMC significantly reduced ($p < 0.001$) the viability of both the MSLN-positive and MSLN-negative cell lines (Fig. 3B, C). Because we observed a cytotoxic effect when treating cells with 200 nM of protein 3.4.4, we used 200 nM of Fn3 protein for subsequent experiments.

Treatment with Fn3 protein induces apoptosis of MSLN-positive cancer cells.

We evaluated the induction of apoptosis on KB-3-1 cells after 3.4.4 treatment, measured by flow cytometry following staining with fluorescently labeled annexin-V and PI (Fig. 4). Annexin V in combination with PI can discriminate between viable cells, early apoptotic cells, late apoptotic cells, and cells in necrosis (Matteucci, Grelli, De Smaele, Fontana, & Mastino, 1999). Cells that are viable and intact do not stain with either annexin V or PI, cells that are in the early stages of apoptosis undergo changes that alter the cell membrane and allow the incorporation of annexin V but still exclude PI, and cells that are in the late stages of apoptosis are stained with both annexin V and PI once PI can penetrate a degrading membrane and intercalate into nucleic acids. Cells that are necrotic but not from apoptosis have a permeable membrane and stain with PI but not with annexin V.

After 48 h of treatment, Fn3 variant 3.4.4 significantly increased the number of apoptotic cells compared to vehicle-treated cells (Fig. 4A, B). The number of early and late apoptotic cells increased from the untreated levels when treated with Fn3 3.4.4 ($p < 0.001$ for increase in early apoptosis, $p < 0.05$ for increase in late apoptosis), and the number of necrotic cells also increased with treatment ($p < 0.001$). Cells treated with the non-binding control Fn3 RDG demonstrated no increase in apoptosis or necrosis compared to vehicle-treated cells (Fig. 4C, D).

Fn3 protein induces apoptosis of MSLN-positive cancer cells in a caspase-independent manner.

We examined whether the observed apoptosis of MSLN-positive tumor cells from variant 3.4.4 treatment was executed via a caspase-mediated pathway. Caspases typically play a key role in apoptosis (Riedl & Shi, 2004; Zhao & Zhang, 2018), therefore we assessed the activity of the executioner caspases, caspases-3 and -7 (Fig. 5). KB-3-1 cells were treated with 3.4.4, Fn3 RDG, or MMC. After 48 h of treatment, caspase 3/7 activities were significantly increased in the MMC-treated cells ($p < 0.001$) compared to vehicle-treated cells, while neither treatment with Fn3 3.4.4 nor negative control Fn3 RDG demonstrated increased caspase activity over vehicle treatment (Fig. 5A).

The biochemical pathways associated with apoptosis, and the time required to detect activation of these different biochemical pathways, are variable and dependent on cell line, specific apoptosis inducer, biochemical events assayed, and the time at which events are

assayed (Elmore, 2007). To confirm 3.4.4 treatment did not induce caspase activation at earlier time points, we monitored caspase-3/7 activities over an extended time course. Compared with vehicle-treated cells, 3.4.4-treated cells showed no increase in caspase-3/7 activities when measured at 6, 12, 24, or 36 h (Fig. 5B).

Decreased cell viability and increased apoptosis is not due to MSLN downregulation.

We investigated whether the observed 3.4.4-induced apoptosis was due to downregulation of surface MSLN. Aberrant signaling via overexpressed receptors is implicated in many cancers and interruption of this process can cause antitumor effects (Richter & Zhang, 2005). Signaling abrogation mechanisms include blocking ligand binding, inhibiting downstream signaling pathways following receptor binding, and receptor downregulation (Friedman et al., 2005; Lee et al., 2003). Ligand-induced endocytosis and degradation of receptor is known to be a significant process by which growth-promoting signals are interrupted (Chan, LaPara, & Yee, 2016; Friedman et al., 2005; Hackel, Neil, White, & Wittrup, 2012; Kearns et al., 2015; Maloney et al., 2003; Marmor & Yarden, 2004; Sachdev, Singh, Fujita-Yamaguchi, & Yee, 2006; Spangler et al., 2010). There is previous evidence that direct reduction of surface levels of MSLN by shRNA or siRNA inhibits cell proliferation, migration, and invasion, and sensitizes cancer cells to chemotherapeutics and induces apoptosis (Bharadwaj et al., 2008, 2011; M.-C. Chang et al., 2009; Wang et al., 2012; Zheng et al., 2012). To examine if MSLN receptor downregulation contributed to the observed decrease in MSLN-positive tumor cell viability and increase in apoptosis following 3.4.4 treatment, we measured levels of MSLN on the surface of treated tumor cells using an antibody recognizing MSLN and flow cytometry. We did not detect any changes in surface levels of MSLN on KB-3-1 tumor cells over a time course of 48 h compared to untreated cells, when cells were treated with either variant 3.4.4 or non-binding negative control Fn3 RDG (Fig. 6), indicating that apoptosis induction was not mediated by receptor downregulation.

Fn3 protein enhances sensitivity of KB-3-1 and OVCAR-3 cells to chemotherapeutic mitomycin C.

We evaluated the combined effect of MSLN-binding Fn3 protein and standard chemotherapeutic MMC on MSLN-positive KB-3-1 cells and OVCAR-3 cells. Having observed that variant 3.4.4 increased MSLN-positive cell apoptosis, but not through caspase activation and not through receptor downregulation, we hypothesized that 3.4.4 may act most directly on survival pathways of the tumor cells, accelerating the apoptosis of cells that were naturally beginning down an apoptosis pathway. If 3.4.4 had this effect of supporting apoptosis, then we hypothesized that treatment of MSLN-positive cells with variant 3.4.4 could increase the sensitivity of cells exposed to a chemotherapeutic agent, when the treatments were administered in combination. Combination therapy has become standard practice in the clinic for cancer therapy (Bayat Mokhtari et al., 2017). Targeting multiple, essential tumor pathways is often more effective than monotherapies, and can promote robust anti-cancer effects while minimizing the likelihood that resistant cancer cells will develop (Bayat Mokhtari et al., 2017; Saputra, Huang, Chen, & Tucker-Kellogg, 2018).

When MSLN-positive KB-3-1 cells were simultaneously treated with MSLN-binding Fn3 protein 3.4.4 and chemotherapeutic MMC, the cancer cells exhibited enhanced sensitivity to MMC compared to KB-3-1 cells treated with either Fn3 3.4.4 or MMC alone (Fig. 7 A, B). The percentage of total apoptotic cells increased significantly when comparing cells treated with 200 nM Fn3 3.4.4 to cells treated with the combination of 1 μ M of MMC and 200 nM of Fn3 3.4.4 ($23 \pm 3\%$ and $62 \pm 3\%$, p-value < 0.001) and when comparing cells treated with 1 μ M of MMC to cells treated with the combination of 1 μ M of MMC and 200 nM of Fn3 3.4.4 ($44 \pm 5\%$ and $62 \pm 3\%$, p-value < 0.01) (Fig. 7B).

To determine if a similar therapeutic effect would be observed for another MSLN-positive tumor cell line, we repeated the combination therapy experiment with OVCAR-3 ovarian carcinoma cells (Fig. 7 C, D), a cell line with a moderate level of MSLN expression (Supporting Information Fig. S1). OVCAR-3 cells provide an interesting comparison to KB-3-1 cells because while KB-3-1 cells do not express CA125, which is a native binding partner for MSLN, the OVCAR-3 cells do express high levels of CA125 (Supporting Information Fig. S1). The percentage of total apoptotic cells increased significantly when comparing cells treated with 200 nM Fn3 3.4.4 to cells treated with 1 μ M of MMC and 200 nM of Fn3 3.4.4 ($35 \pm 1\%$ and $71 \pm 7\%$, p-value < 0.001) and when comparing cells treated with 1 μ M of MMC to cells treated with 1 μ M of MMC and 200 nM of Fn3 3.4.4 ($42 \pm 2\%$ and $71 \pm 7\%$, p-value < 0.01) (Fig. 7D).

These results highlight the potential of targeting MSLN with biologic therapeutics in combination therapy with traditional chemotherapeutics for more selective, synergistic treatment of tumors expressing MSLN. Such combination therapy can allow a reduction in chemotherapeutic dose, reducing the nonspecific toxic side effects of non-selective cytotoxic agents. Building on the recent successes of antibody-drug conjugates, one promising approach is to create a protein-drug conjugate, coupling a chemotherapeutic to an engineered Fn3 variant that targets MSLN, merging targeted drug delivery with combination therapy and further reducing nonspecific toxicities. We anticipate that the highly stable structure of the Fn3 scaffold and the lack of native disulfide bonds will facilitate the development of strategies to synthesize Fn3-drug conjugates for targeted combination therapy of MSLN-positive tumors.

CONCLUSION

In summary, we have successfully engineered a non-antibody Fn3 protein that binds cancer antigen MSLN with high affinity and specificity, and has a targeted therapeutic effect on MSLN-positive tumor cells, reducing cell viability and increasing apoptosis. Further, the Fn3 protein engineered to bind MSLN increases the sensitivity of tumor cells to a common chemotherapeutic agent when used as a combination therapy. In recently reported work, treatment with anetumab ravtansine, a MSLN-specific antibody-drug conjugate, not only inhibited tumor growth in ovarian cancer models as a monotherapy, but also exhibited an additive effect when used in combination with targeted agents and standard chemotherapeutics (Quanz et al., 2018). Together, this current report and the recent results of related research validate that molecules developed to target MSLN are promising for both

monotherapy and combination therapy for patients who do not currently have any targeted treatment options.

Interestingly, the apoptosis of KB-3-1 cells induced by the non-antibody Fn3 variant 3.4.4 does not occur via caspase activation, and we do not observe downregulation of levels of MSLN on the tumor cell surface of KB-3-1 cells following treatment with 3.4.4. The absence of these commonly observed pathways for targeted treatment of tumor cells suggests that a currently unknown alternate pathway is engaged in the KB-3-1 tumor cell response to variant Fn3 3.4.4. Future research exploring relevant pathways for 3.4.4-induced tumor cell death, in the tumor cell lines used in this paper and in other cell lines expressing MSLN, has the potential to uncover and further elucidate important signaling pathways for MSLN-positive tumor cells, informing ongoing efforts to design effective targeted treatments for patients with tumors expressing MSLN. We are also interested in working to understand if and how Fn3 3.4.4 may modulate the interaction of MSLN and native binding partner CA125, building on our observation that OVCAR-3 cells had enhanced response to 3.4.4 treatment alone compared to the 3.4.4 treatment response of KB-3-1 cells. This difference in response could be related to potential disruption of MSLN and CA125 interactions by 3.4.4, which would only be relevant for the MSLN+/CA125+ OVCAR-3 cells. Combination therapy with molecules targeting MSLN and molecules targeting CA125 is another approach warranting further study.

Supplementary Material

Refer to Web version on PubMed Central for supplementary material.

ACKNOWLEDGEMENTS

This work was funded by National Institutes of Health grant R15CA198927-01 (SJM). DAD was supported by a Smith College McKinley Honors Fellowship and the Tomlinson Memorial Fund. We thank Dr. Amy Burnside, Director of the University of Massachusetts Amherst Flow Cytometry Core Facility; Lou Ann Bierwert, Director of the Smith College Center for Molecular Biology; and Dr. Kalina Dimova, Director of the Smith College Center for Proteomics for expert insight and technical assistance. We acknowledge Dr. Sallie Smith-Schneider at the Pioneer Valley Life Sciences Institute for insightful discussions and providing the T-47D cell line, Dr. Mitchell Ho and Dr. Michael Gottesman of the National Cancer Institute for providing A431/H9 and KB-3-1 cell lines, and Dr. Benjamin Hackel at the University of Minnesota for providing the naive Gr2 Fn3 yeast display library and related plasmid DNA.

Funding Information

National Institutes of Health, Grant R15CA198927-01.

REFERENCES

- Adusumilli PS, Cherkassky L, Villena-Vargas J, Colovos C, Servais E, Plotkin J, ... Sadelain M (2014). Regional delivery of mesothelin-targeted CAR T cell therapy generates potent and long-lasting CD4-dependent tumor immunity. *Science Translational Medicine*, 6(261), 261ra151–261ra151. 10.1126/scitranslmed.3010162
- Argani P, Iacobuzio-donahue C, Ryu B, Rosty C, Goggins M, Wilentz RE, ... Hruban RH (2001). Mesothelin is overexpressed in the vast majority of ductal adenocarcinomas of the pancreas: Identification of a new pancreatic cancer marker by serial analysis of gene expression (SAGE). *Clinical Cancer Research*, 7, 3862–3868. [PubMed: 11751476]

- Bayat Mokhtari R, Homayouni TS, Baluch N, Morgatskaya E, Kumar S, Das B, & Yeger H (2017). Combination therapy in combating cancer. *Oncotarget*, 8(23), 38022–38043. 10.18632/oncotarget.16723 [PubMed: 28410237]
- Bayoglu I, Kucukzeybek B, Kucukzeybek Y, Varol U, Yildiz I, Alacacioglu A, ... Tarhan M (2015). Prognostic value of mesothelin expression in patients with triple negative and HER2-positive breast cancers. *Biomedicine and Pharmacotherapy*, 70, 190–195. [PubMed: 25776500]
- Bera TK, & Pastan I (2000). Mesothelin Is Not Required for Normal Mouse Development or Reproduction. *Molecular and Cellular Biology*, 20(8), 2902–2906. [PubMed: 10733593]
- Bharadwaj U, Li M, Chen C, & Yao Q (2008). Mesothelin-induced pancreatic cancer cell proliferation involves alteration of cyclin E via activation of signal transducer and activator of transcription protein 3. *Molecular Cancer Research: MCR*, 6(11), 1755–1765. 10.1158/1541-7786.MCR-08-0095 [PubMed: 19010822]
- Bharadwaj U, Marin-muller C, Li M, Chen C, & Yao Q (2011). Mesothelin confers pancreatic cancer cell resistance to TNF- α -induced apoptosis through Akt / PI3K / NF- κ B activation and IL-6 / Mcl-1 overexpression. *Molecular Cancer*, 10(106). 10.1186/1476-4598-10-106
- Boder ET, & Wittrup KD (1997). Yeast surface display for screening combinatorial polypeptide libraries. *Nature Biotechnology*, 15, 553–557. 10.1038/nm0798-822
- Chan JY, LaPara K, & Yee D (2016). Disruption of insulin receptor function inhibits proliferation in endocrine-resistant breast cancer cells. *Oncogene*, 35(32), 4235–4243. 10.1038/ncr.2015.488 [PubMed: 26876199]
- Chang K, & Pastan I. (1996). Molecular cloning of mesothelin, a differentiation antigen present on mesothelium, mesotheliomas, and ovarian cancers. *PNAS*, 93, 136–140. 10.1073/pnas.93.1.136 [PubMed: 8552591]
- Chang Kai, Pastan I, & Willingham MC (1992). Isolation and characterization of monoclonal antibody, K1, reactive with ovarian cancers and normal mesothelium. *International Journal of Cancer*, 50(3), 373–381. 10.1002/ijc.2910500308 [PubMed: 1735605]
- Chang M-C, Chen C-A, Hsieh C-Y, Lee C-N, Su Y-N, Hu Y-H, & Cheng W-F (2009). Mesothelin inhibits paclitaxel-induced apoptosis through the PI3K pathway. *Biochemical Journal*, 424(3), 449–458. 10.1042/bj20082196 [PubMed: 19747165]
- Chen S-H, Hung W-C, Wang P, Paul C, & Konstantopoulos K (2013). Mesothelin binding to CA125/MUC16 promotes pancreatic cancer cell motility and invasion via MMP-7 activation. *Nature Scientific Reports*, 3(1870). 10.1038/srep01870
- Cheng W-F, Huang C-Y, Chang M-C, Hu Y-H, Chiang Y-C, Chen Y-L, ... Chen C-A (2009). High mesothelin correlates with chemoresistance and poor survival in epithelial ovarian carcinoma. *British Journal of Cancer*, 100(7), 1144–1153. 10.1038/sj.bjc.6604964 [PubMed: 19293794]
- Comamala M, Pinard M, Thériault C, Matte I, Albert A, Boivin M, ... Rancourt C (2011). Downregulation of cell surface CA125/MUC16 induces epithelial-to-mesenchymal transition and restores EGFR signalling in NIH:OVCAR3 ovarian carcinoma cells. *British Journal of Cancer*, 104(6), 989–999. 10.1038/bjc.2011.34 [PubMed: 21326240]
- El-Behaedi S, Landsman R, Rudloff M, Kolyvas E, Albalawy R, Zhang X, ... Alewine C (2018). Protein Synthesis Inhibition Activity of Mesothelin Targeting Immunotoxin LMB-100 Decreases Concentrations of Oncogenic Signaling Molecules and Secreted Growth Factors. *Toxins*, 10(11), 447–447. 10.3390/toxins10110447
- Elmore S. (2007). Apoptosis: A review of programmed cell death. *Toxicologic Pathology*, 35(4), 495–516. 10.1080/01926230701320337 [PubMed: 17562483]
- Fiedler M, & Skerra A (2014). Non-Antibody Scaffolds as Alternative Therapeutic Agents In Dübel S & Reichert JM (Eds.), *Handbook of Therapeutic Antibodies* (pp. 435–474). 10.1002/9783527682423.ch17
- Friedman LM, Rinon A, Schechter B, Lyass L, Lavi S, Bacus SS, ... Yarden Y (2005). Synergistic down-regulation of receptor tyrosine kinases by combinations of mAbs: Implications for cancer immunotherapy. *Proceedings of the National Academy of Sciences of the United States of America*, 102(6), 1915–1920. 10.1073/pnas.0409610102 [PubMed: 15684082]
- Golfier S, Kopitz C, Kahnert A, Heisler I, Schatz CA, Stelte-Ludwig B, ... Ziegelbauer K (2014). Anetumab Ravtansine: A novel mesothelin-targeting antibody–drug conjugate cures tumors with

- heterogeneous target expression favored by bystander effect. *Molecular Cancer Therapeutics*, 13(6), 1537–1548. 10.1158/1535-7163.MCT-13-0926 [PubMed: 24714131]
- Gubbels JAA, Belisle J, Onda M, Rancourt C, Migneault M, Ho M, ... Patankar MS (2006). Mesothelin-MUC16 binding is a high affinity, N-glycan dependent interaction that facilitates peritoneal metastasis of ovarian tumors. *Molecular Cancer*, 5(1), 50–50. 10.1186/1476-4598-5-50 [PubMed: 17067392]
- Hackel BJ, Neil JR, White FM, & Wittrup KD (2012). Epidermal growth factor receptor downregulation by small heterodimeric binding proteins. *Protein Engineering, Design and Selection*, 25(2), 47–57. 10.1093/protein/gzr056
- Hassan R, Bera T, & Pastan I (2004). Mesothelin: A new target for immunotherapy. *Clinical Cancer Research*, 10, 3937–3942. [PubMed: 15217923]
- Hassan R, Thomas A, Alewine C, Le DT, Jaffee EM, & Pastan I (2016). Mesothelin immunotherapy for cancer: Ready for prime time? *Journal of Clinical Oncology*, 34(34), 4171–4179. 10.1200/JCO.2016.68.3672 [PubMed: 27863199]
- Hilliard T (2018). The Impact of Mesothelin in the Ovarian Cancer Tumor Microenvironment. *Cancers*, 10(9), 277–277. 10.3390/cancers10090277
- Ho M, Hassan R, Zhang J, Wang Q, Onda M, Bera T, & Pastan I (2005). Humoral immune response to mesothelin in mesothelioma and ovarian cancer patients. *Clinical Cancer Research*, 11(10), 3814–3820. 10.1158/1078-0432.CCR-04-2304 [PubMed: 15897581]
- Ho Mitchell, Bera TK, Willingham MC, Ho M, Bera TK, Willingham MC, ... Pastan I (2007). Mesothelin expression in human lung cancer. *Clinical Cancer Research*, 13(5), 1571–1575. 10.1158/1078-0432.CCR-06-2161 [PubMed: 17332303]
- Ho Mitchell, Feng M, Fisher RJ, Rader C, & Pastan I (2011). A novel high-affinity human monoclonal antibody to mesothelin. *International Journal of Cancer*, 128(9), 2020–2030. 10.1002/ijc.25557 [PubMed: 20635390]
- Kachala SS, Bograd AJ, Villena-Vargas J, Suzuki K, Servais EL, Kadota K, ... Adusumilli PS (2014). Mesothelin overexpression is a marker of tumor aggressiveness and is associated with reduced recurrence-free and overall survival in early-stage lung adenocarcinoma. *Clinical Cancer Research*, 20(4), 1020–1028. 10.1158/1078-0432.CCR-13-1862 [PubMed: 24334761]
- Kearns JD, Bukhalid R, Sevecka M, Tan G, Gerami-Moayed N, Werner SL, ... Wolf BB (2015). Enhanced Targeting of the EGFR Network with MM-151, an Oligoclonal Anti-EGFR Antibody Therapeutic. *Molecular Cancer Therapeutics*, 14(7), 1625–1636. 10.1158/1535-7163.MCT-14-0772 [PubMed: 25911688]
- Keydar I, Chen L, Karby S, Weiss F, Delarea J, Radu M, ... Brenner H (1979). Establishment and characterization of a cell line of human breast carcinoma origin. *European Journal of Cancer*, 15(5), 659–670. [PubMed: 228940]
- Koide A, Bailey CW, Huang X, & Koide S (1998). The fibronectin type III domain as a scaffold for novel binding proteins. *Journal of Molecular Biology*, 284(4), 1141–1151. 10.1006/jmbi.1998.2238 [PubMed: 9837732]
- Lee AV, Schiff R, Cui X, Sachdev D, Yee D, Gilmore AP, ... Hadsell DL (2003). New Mechanisms of Signal Transduction Inhibitor Action: Receptor Tyrosine Kinase Down-Regulation and Blockade of Signal Transactivation. *Clinical Cancer Research*, 9(1), 516s–523s. [PubMed: 12538509]
- Maloney EK, McLaughlin JL, Dagdigian NE, Garrett LM, Connors KM, Zhou X-M, ... Singh R (2003). An Anti-Insulin-like Growth Factor I Receptor Antibody That Is a Potent Inhibitor of Cancer Cell Proliferation. *Cancer Research*, 63(16), 5073–5083. [PubMed: 12941837]
- Marmor MD, & Yarden Y (2004). Role of protein ubiquitylation in regulating endocytosis of receptor tyrosine kinases. *Oncogene*, 23(11), 2057–2070. 10.1038/sj.onc.1207390 [PubMed: 15021893]
- Matteucci C, Grelli S, De Smaele E, Fontana C, & Mastino A (1999). Identification of nuclei from apoptotic, necrotic, and viable lymphoid cells by using multiparameter flow cytometry. *Cytometry*, 35(2), 145–153. [PubMed: 10554170]
- Moore SJ, Leung CL, & Cochran JR (2012). Knottins: Disulfide-bonded therapeutic and diagnostic peptides. *Drug Discovery Today: Technologies*, 9(1), e3–e11. 10.1016/j.ddtec.2011.07.003
- Morello A, Sadelain M, & Adusumilli PS (2016). Mesothelin-Targeted CARs: Driving T Cells to Solid Tumors. *Cancer Discovery*, 6(2), 133–146. 10.1158/2159-8290.CD-15-0583 [PubMed: 26503962]

- Ordóñez NG (2003). Application of mesothelin immunostaining in tumor diagnosis. *The American Journal of Surgical Pathology*, 27(11), 1418–1428. [PubMed: 14576474]
- Parinyanitikul N, Blumenschein GR, Wu Y, Lei X, Chavez-Macgregor M, Smart M, & Gonzalez-Angulo AM (2013). Mesothelin expression and survival outcomes in triple receptor negative breast cancer. *Clinical Breast Cancer*, 13(5), 378–384. 10.1016/j.clbc.2013.05.001 [PubMed: 23810431]
- Pastan I, & Hassan R (2014). Discovery of mesothelin and exploiting it as a target for immunotherapy. *Cancer Research*, 74(11), 2907–2912. 10.1158/0008-5472.CAN-14-0337 [PubMed: 24824231]
- Quanz M, Hagemann UB, Zitzmann-Kolbe S, Stelte-Ludwig B, Golfier S, Elbi C, ... Schatz CA (2018). Anetumab ravtansine inhibits tumor growth and shows additive effect in combination with targeted agents and chemotherapy in mesothelin-expressing human ovarian cancer models. *Oncotarget*, 9(75), 34103–34121. 10.18632/oncotarget.26135 [PubMed: 30344925]
- Richter M, & Zhang H (2005). Receptor-Targeted Cancer Therapy. *DNA and Cell Biology*, 24(5), 271–282. 10.1089/dna.2005.24.271 [PubMed: 15869404]
- Riedl SJ, & Shi Y (2004). Molecular mechanisms of caspase regulation during apoptosis. *Nature Reviews Molecular Cell Biology*, 5(11), 897–907. 10.1038/nrm1496 [PubMed: 15520809]
- Rump A, Morikawa Y, Minami S, Umesaki N, Takeuchi M, & Miyajima A (2004). Binding of Ovarian Cancer Antigen Cell Adhesion Binding of Ovarian Cancer Antigen CA125 / MUC16 to Mesothelin Mediates Cell Adhesion. *The Journal of Biological Chemistry*, 279, 9190–9198. 10.1074/jbc.M312372200 [PubMed: 14676194]
- Sachdev D, Singh R, Fujita-Yamaguchi Y, & Yee D (2006). Down-regulation of Insulin Receptor by Antibodies against the Type I Insulin-Like Growth Factor Receptor: Implications for Anti-Insulin-Like Growth Factor Therapy in Breast Cancer. *Cancer Research*, 66(4), 2391–2402. 10.1158/0008-5472.CAN-05-3126 [PubMed: 16489046]
- Saputra EC, Huang L, Chen Y, & Tucker-Kellogg L (2018). Combination Therapy and the Evolution of Resistance: The Theoretical Merits of Synergism and Antagonism in Cancer. *Cancer Research*, 78(9), 2419–2431. 10.1158/0008-5472.CAN-17-1201 [PubMed: 29686021]
- Servais EL, Colovos C, Rodriguez L, Bograd AJ, Nitadori J, Sima C, ... Adusumilli PS (2012). Mesothelin overexpression promotes mesothelioma cell invasion and MMP-9 secretion in an orthotopic mouse model and in epithelioid pleural mesothelioma patients. *Clinical Cancer Research: An Official Journal of the American Association for Cancer Research*, 18(9), 2478–2489. 10.1158/1078-0432.CCR-11-2614 [PubMed: 22371455]
- Shen DW, Cardarelli C, Hwang J, Cornwell M, Richert N, Ishii S, ... Gottesman MM (1986). Multiple drug-resistant human KB carcinoma cells independently selected for high-level resistance to colchicine, adriamycin, or vinblastine show changes in expression of specific proteins. *Journal of Biological Chemistry*, 261(17), 7762–7770. [PubMed: 3711108]
- Shimizu A, Hirono S, Tani M, Kawai M, Okada KI, Miyazawa M, ... Yamaue H (2012). Coexpression of MUC16 and mesothelin is related to the invasion process in pancreatic ductal adenocarcinoma. *Cancer Science*, 103(4), 739–746. 10.1111/j.1349-7006.2012.02214.x [PubMed: 22320398]
- Simeon R, & Chen Z (2018). In vitro-engineered non-antibody protein therapeutics. *Protein & Cell*, 9(1), 3–14. 10.1007/s13238-017-0386-6 [PubMed: 28271446]
- Sirois AR, Deny DA, Baierl SR, George KS, & Moore SJ (2018). Fn3 proteins engineered to recognize tumor biomarker mesothelin internalize upon binding. *PLoS ONE*, 13(5), e0197029–e0197029. 10.1371/journal.pone.0197029 [PubMed: 29738555]
- Spangler JB, Neil JR, Abramovitch S, Yarden Y, White FM, Lauffenburger DA, & Wittrup KD (2010). Combination antibody treatment down-regulates epidermal growth factor receptor by inhibiting endosomal recycling. *Proceedings of the National Academy of Sciences of the United States of America*, 107(30), 13252–13257. 10.1073/pnas.0913476107 [PubMed: 20616078]
- Tang Z, Feng M, Gao W, Phung Y, Chen W, Chaudhary A, ... Ho M (2013). A human single-domain antibody elicits potent antitumor activity by targeting an epitope in mesothelin close to the cancer cell surface. *Molecular Cancer Therapeutics*, 12, 416–426. 10.1158/1535-7163.MCT-12-0731 [PubMed: 23371858]
- Tang Zhewei, Qian M, & Ho M (2013). The role of mesothelin in tumor progression and targeted therapy. *Anticancer Agents Med Chem*, 13(2), 276–280. [PubMed: 22721387]

- Tchou J, Wang LC, Selven B, Zhang H, Conejo-Garcia J, Borghaei H, ... Zhang PJ (2012). Mesothelin, a novel immunotherapy target for triple negative breast cancer. *Breast Cancer Research and Treatment*, 133, 799–804. 10.1007/s10549-012-2018-4 [PubMed: 22418702]
- Thomas A, Chen Y, Steinberg SM, Luo J, Pack S, Abdullaev Z, ... Giaccone G (2015). High mesothelin expression in advanced lung adenocarcinoma is associated with KRAS mutations and a poor prognosis. *Oncotarget*, 6(13), 11694–11703. 10.18632/oncotarget.3429 [PubMed: 26028668]
- Uehara N, Matsuoka Y, & Tsubura A (2008). Mesothelin promotes anchorage-independent growth and prevents anoikis via extracellular signal-regulated kinase signaling pathway in human breast cancer cells. *Molecular Cancer Research*, 6(2), 186–193. 10.1158/1541-7786.MCR-07-0254 [PubMed: 18245228]
- Vazquez-Lombardi R, Phan TG, Zimmermann C, Lowe D, Jeremias L, & Christ D (2015). Challenges and opportunities for non-antibody scaffold drugs. *Drug Discovery Today*, 20(10), 1271–1283. 10.1016/j.drudis.2015.09.004 [PubMed: 26360055]
- Wang K, Bodempudi V, Liu Z, Borrego-diaz E, Yamoutpoor F, Meyer A, ... Olyaei MS (2012). Inhibition of Mesothelin as a Novel Strategy for Targeting Cancer Cells. *PLoS ONE*, 7(4), e33214–e33214. 10.1371/journal.pone.0033214 [PubMed: 22485139]
- Woldring DR, Holec PV, Zhou H, & Hackel BJ (2015). High-throughput ligand discovery reveals a sitewise gradient of diversity in broadly evolved hydrophilic fibronectin domains. *PLoS ONE*, 10(9), 1–29. 10.1371/journal.pone.0138956
- Yu L, Feng M, Kim H, Phung Y, Kleiner DE, Gores GJ, ... Ho M (2010). Mesothelin as a potential therapeutic target in human cholangiocarcinoma. *Journal of Cancer*, 1, 141–149. [PubMed: 20922056]
- Zhang Y, & Pastan I (2012). Modulating mesothelin shedding to improve therapy. *Oncotarget*, 3(2), 114–115. [PubMed: 22337812]
- Zhang Y, Xiang L, Hassan R, & Pastan I (2007). Immunotoxin and Taxol synergy results from a decrease in shed mesothelin levels in the extracellular space of tumors. *PNAS*, 104(43), 17099–17104. [PubMed: 17940013]
- Zhao H, & Zhang L (2018). MUC16 mutation predicts favorable clinical outcome and correlates decreased Warburg effect in gastric cancer. *Biochemical and Biophysical Research Communications*, 506(4), 780–786. [PubMed: 30389134]
- Zheng C, Jia W, Tang Y, Zhao H, Jiang Y, & Sun S (2012). Mesothelin regulates growth and apoptosis in pancreatic cancer cells through p53-dependent and -independent signal pathway. *Journal of Experimental & Clinical Cancer Research*, 31(1), 84. 10.1186/1756-9966-31-84 [PubMed: 23034174]

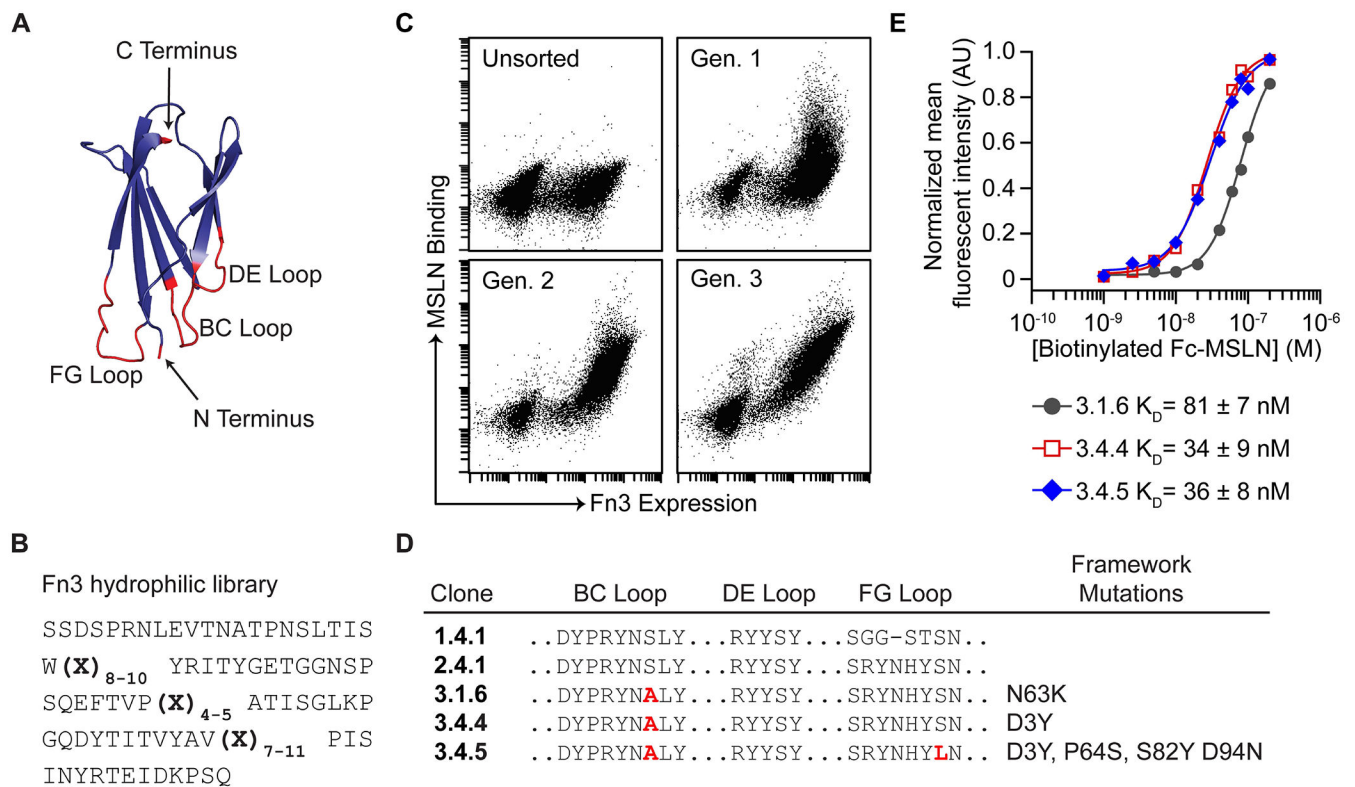


Figure 1. Engineering and characterization of a third generation anti-mesothelin Fn3 library. (A) The human fibronectin type III (Fn3) protein scaffold has a highly stable structure with loops that are suitable for mutation to engineer novel molecular recognition properties (PDB 1TTG). (B) The Fn3 library sequence (Woldring et al., 2015). (C) Indicated yeast libraries displaying Fn3 variants were labeled with an antibody to a terminal c-myc epitope tag and 25 nM biotinylated, Fc-tagged MSLN. Unsorted refers to the original naïve library. Generation 1 refers to the library following four rounds of FACS. Generation 2 refers to the library following one round of mutagenic PCR and four rounds of FACS. Generation 3 refers to the library that has undergone mutagenic PCR twice, with four rounds of FACS. (D) Selected clones from a third generation library demonstrate further evolved sequences when compared to our previously reported clones. (E) Individual clones were displayed on the surface of yeast and incubated with a range of concentrations of biotinylated, Fc-tagged MSLN. Experimental triplicate data were collected, and the dissociation constant is reported as the mean \pm SD of the K_D values calculated for each replicate. A representative binding curve is shown for each variant.

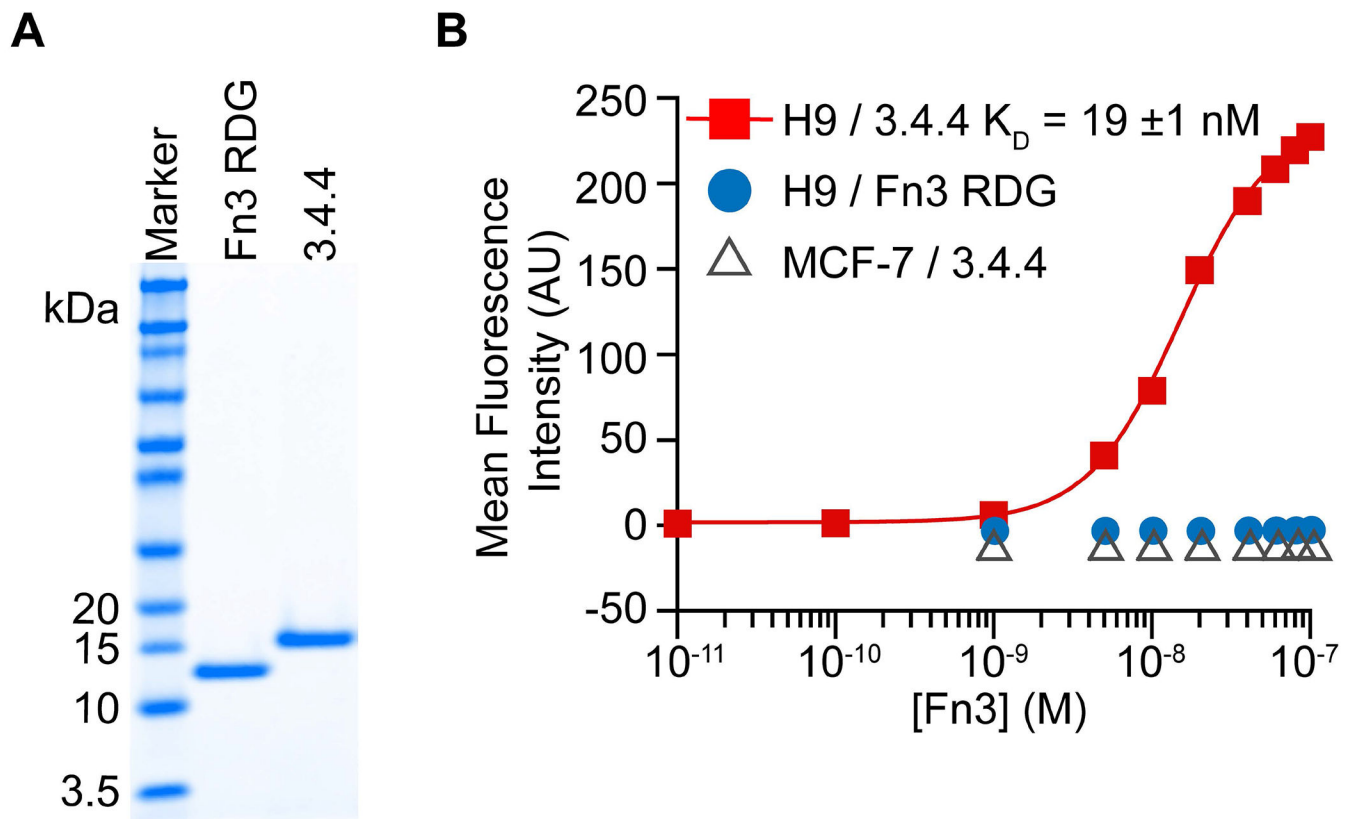


Figure 2. Fn3 protein variant 3.4.4 selectively binds tumor cell-surface MSLN with high affinity. (A) Engineered Fn3 clone 3.4.4 and Fn3 RDG were expressed in bacteria and purified to high purity (>99%) as analyzed by SDS-PAGE. Fn3 3.4.4 expected molecular weight: 13 kDa, Fn3 RDG expected molecular weight: 11 kDa. (B) Binding of 3.4.4 and Fn3-RDG to cell surface MSLN were measured using equilibrium binding assays. H9 cells express MSLN, MCF-7 cells do not express MSLN. The assays were performed as experimental triplicates. Data from each replicate were fit to a sigmoidal curve, and a K_D value was calculated as the concentration yielding the half-maximal value. The K_D is reported as the mean \pm SD. Representative binding curves are shown.

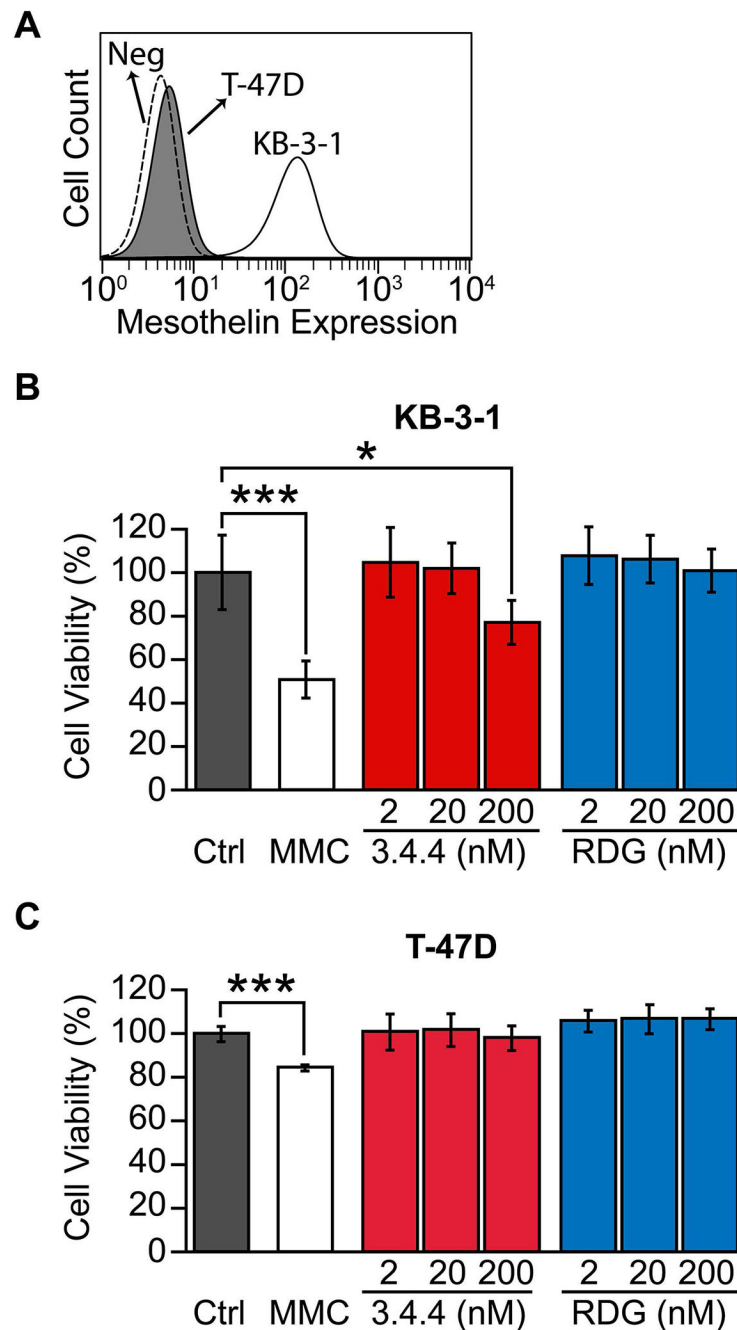


Figure 3. Fn3 protein decreases the viability of MSLN-positive cancer cells.

(A) Analysis by flow cytometry confirms MSLN presence on the surface of KB-3-1 cells (white histogram, solid line) as detected by an anti-MSLN antibody. The T-47D cell line does not express MSLN (gray histogram, solid line). Dashed line, unstained T-47D cells. (B) KB-3-1 and (C) T-47D cells were treated with various concentrations of 3.4.4, Fn3 RDG, or MMC for 48 h. Treated cells were subjected to a CCK-8 assay to measure cell viability, which was normalized to vehicle-treated cells. Error bars indicate mean \pm SD ($n = 9$); * $p < 0.05$, *** $p < 0.001$ as determined with an unpaired Student's two-tailed t -test.

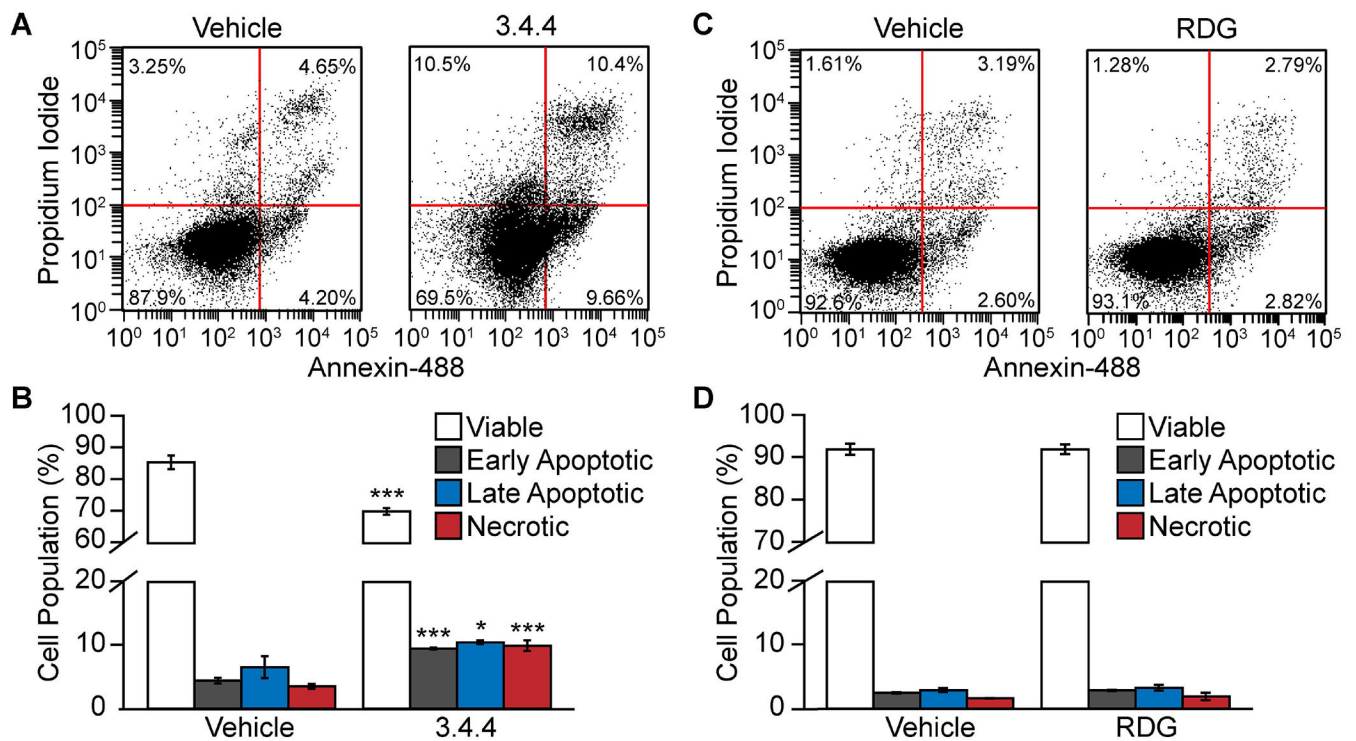


Figure 4. Fn3 protein induces apoptosis in MSLN-positive cancer cells.

Induction of apoptosis of KB-3-1 cells following Fn3 3.4.4 treatment was evaluated by staining with annexin-V and PI. (A, C) KB-3-1 cells were treated with 3.4.4 or Fn3 RDG, then stained with annexin-V AF488 and PI and analyzed by flow cytometry. A representative plot of each treatment is shown. Viable cells (annexin-V⁻/PI⁻) are in the lower left quadrant, early apoptotic cells (annexin-V⁺/PI⁻) are in the lower right quadrant, late apoptotic cells (annexin-V⁺/PI⁺) are in the upper right quadrant, and necrotic cells (annexin-V⁻/PI⁺) are in the upper left quadrant. Vehicle varies slightly between two treatments, and each vehicle control is shown separately. (B, D) Quantitative analysis of induction of apoptosis and necrosis after treatments. Data are presented as the mean \pm SD ($n = 3$). * $p < 0.05$, *** $p < 0.001$ as determined with an unpaired Student's two-tailed t -test.

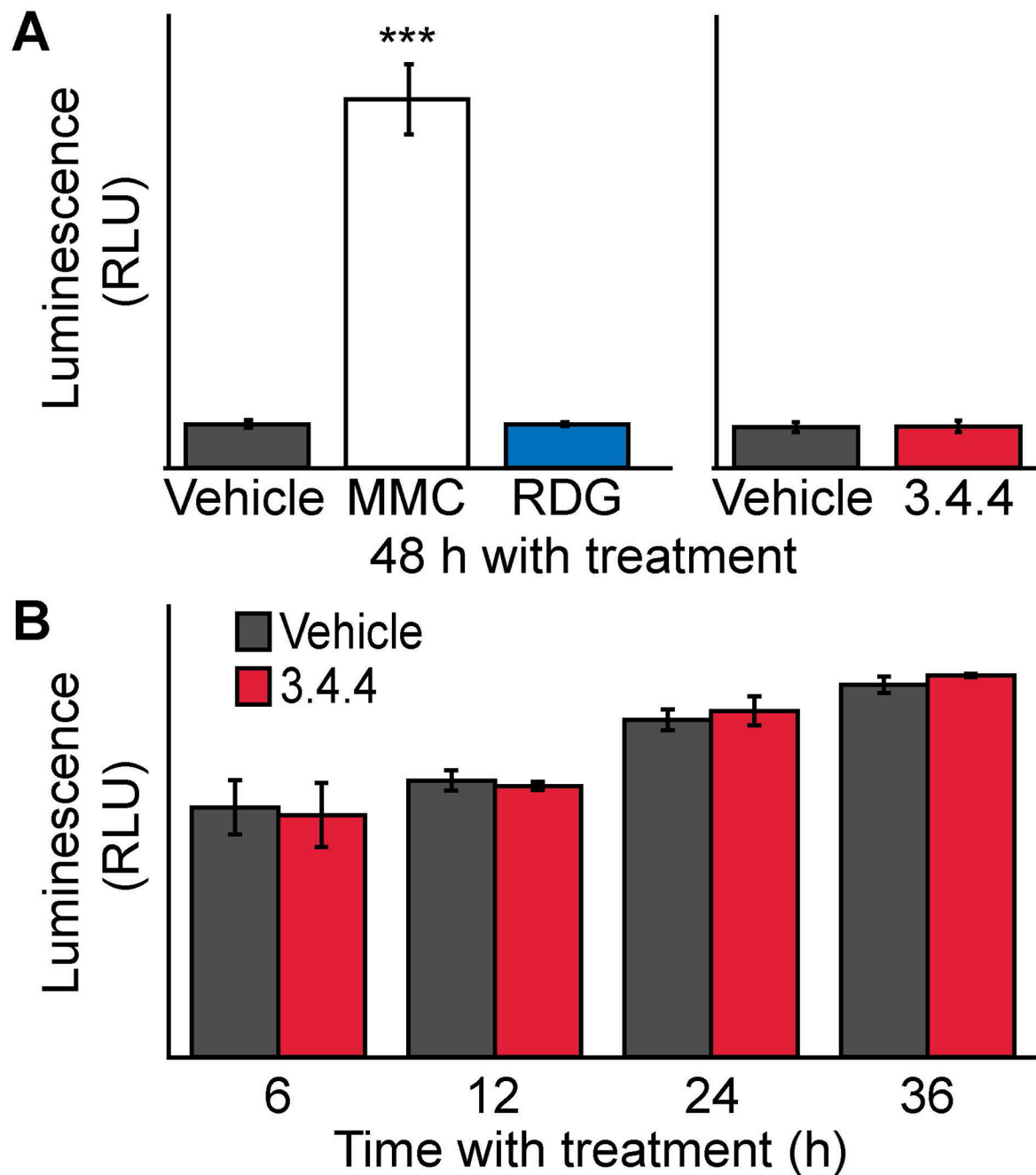


Figure 5. Analysis of caspase 3/7 activation in MSLN-positive cells treated with Fn3 protein. (A) KB-3-1 cells were treated with 3.4.4, Fn3 RDG, or MMC for 48 h, and caspase 3/7 activation was analyzed. Positive control chemotherapeutic MMC induced caspase activation, while Fn3 3.4.4 and negative control Fn3 RDG did not activate caspases. Error bars indicate mean \pm SD (n = 9). *** $p < 0.001$ as determined with an unpaired Student's two-tailed t -test. (B) Treatment of KB-3-1 cells with Fn3 3.4.4 also did not activate caspase 3/7 over the indicated time points. Error bars indicate mean \pm SD (n = 3).

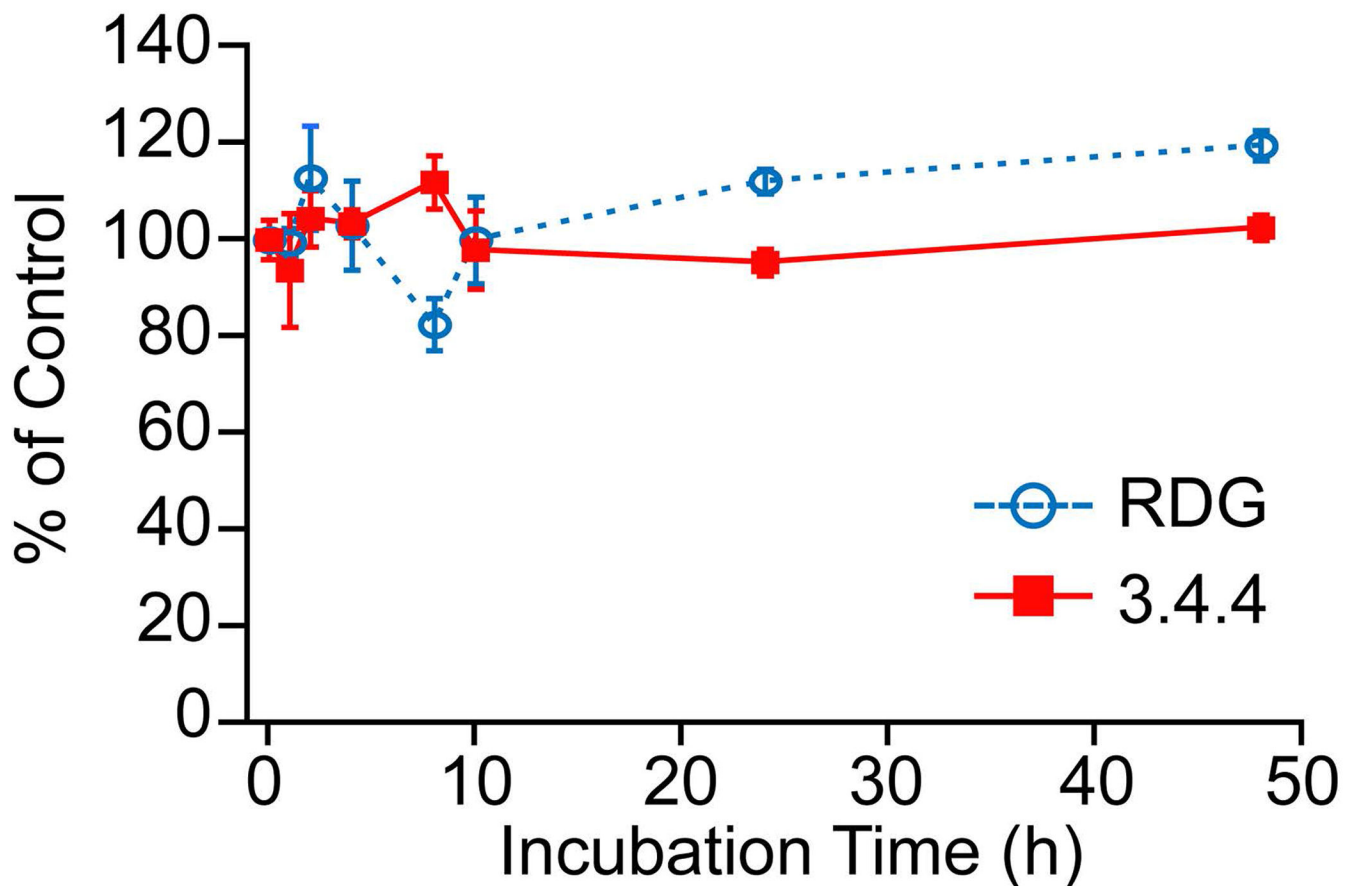


Figure 6. Surface MSLN expression is not downregulated following treatment with Fn3 variant 3.4.4.

KB-3-1 cells that express MSLN were incubated with 3.4.4 (square) or Fn3 RDG (circle). At the specified time points, surface MSLN was quantified via flow cytometry with an antibody that binds MSLN. Surface MSLN levels relative to untreated KB-3-1 cells are plotted as a function of time. Error bars indicate mean \pm SD ($n = 3$). No significant downregulation of surface MSLN was observed, as determined with an unpaired Student's two-tailed t -test.

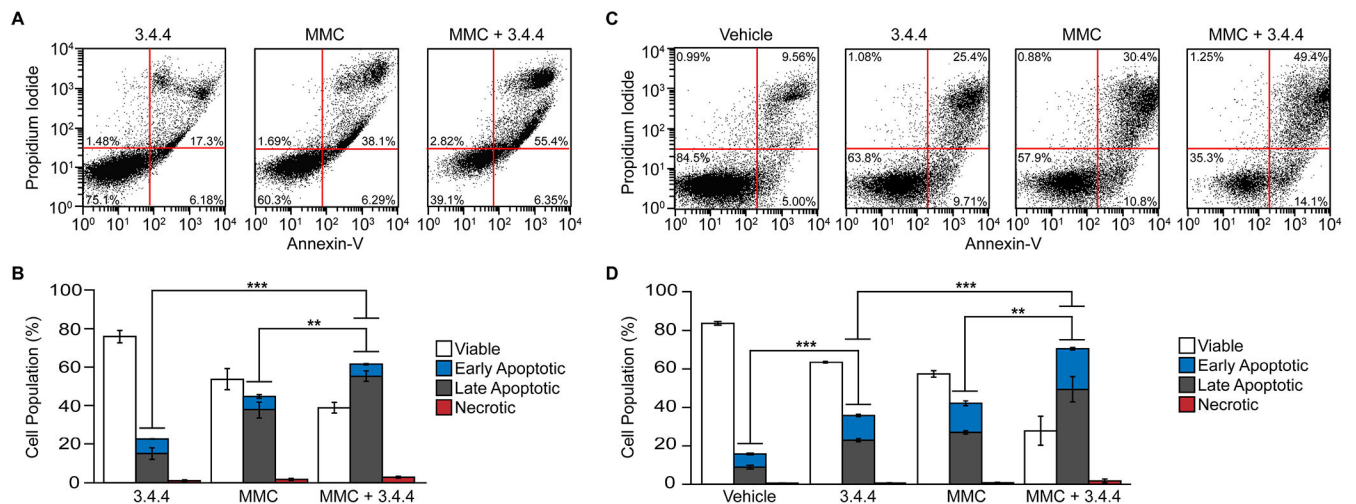


Figure 7. Treatment with Fn3 variant 3.4.4 enhances sensitivity of KB-3-1 cells and OVCAR-3 cells to chemotherapeutic.

Induction of apoptosis of KB-3-1 cells and OVCAR-3 cells following treatment with 3.4.4, MMC, or MMC in combination with Fn3 3.4.4 was evaluated by staining with annexin-V and PI. (A) KB-3-1 and (C) OVCAR-3 cells were treated with 200 nM Fn3 3.4.4, 1 μ M MMC, or 1 μ M MMC and 200 nM Fn3 3.4.4, then stained with annexin-V AF488 and PI and analyzed by flow cytometry. A representative plot of each treatment is shown. Viable cells (annexin-V⁻/PI⁻) are in the lower left quadrant, early apoptotic cells (annexin-V⁺/PI⁻) are in the lower right quadrant, late apoptotic cells (annexin-V⁺/PI⁺) are in the upper right quadrant, and necrotic cells (annexin-V⁻/PI⁺) are in the upper left quadrant. (B, D) Quantitative analysis of induction of apoptosis in (B) KB-3-1 cells and (D) OVCAR-3 cells after treatments. Data are presented as the mean \pm SD (n = 3). ** $p < 0.01$, *** $p < 0.001$ as determined with an unpaired Student's two-tailed t -test.